

# Hydrogen Bonding Interactions and Miscibility Between Phenolic Resin and Octa(acetoxystyryl) Polyhedral Oligomeric Silsesquioxane (AS-POSS) Nanocomposites

SHIAO-WEI KUO,<sup>1</sup> HAN-CHING LIN,<sup>1</sup> WU-JANG HUANG,<sup>2</sup> CHIH-FENG HUANG,<sup>1</sup> FENG-CHIH CHANG<sup>1</sup>

<sup>1</sup>Institute of Applied Chemistry, National Chiao Tung University, Hsin Chu, Taiwan, Republic of China

<sup>2</sup>Department of Environmental Science and Engineering, National Ping-Tung University of Science and Technology, Ping-Tun, Taiwan, Republic of China

Received 15 June 2005; accepted 20 November 2005

DOI: 10.1002/polb.20731

Published online in Wiley InterScience (www.interscience.wiley.com).

**ABSTRACT:** We have synthesized a polyhedral oligomeric silsesquioxane (POSS) derivative containing eight acetoxystyryl functional groups [octa(acetoxystyryl)octasil-sesquioxane (AS-POSS)] and then blended it with phenolic resin to form nanocomposites stabilized through hydrogen bonding interactions between the phenolic resin's hydroxyl group and the AS-POSS derivative's carbonyl and siloxane groups. One- and two-dimensional infrared spectroscopy analyses provided positive evidence for these types of hydrogen bonding interactions. In addition, we calculated the interassociation equilibrium constant, based on the Painter–Coleman association model (PCAM), between phenolic resin and POSS indirectly from the fraction of hydrogen-bonded carbonyl groups; quantitative analyses indicate that the hydroxyl–siloxane interassociation from the PCAM is entirely consistent with the classical Coggeshall and Saier (C and S) methodology. From a thermal analysis, we observed that the miscibility between phenolic and AS-POSS occurs at a relatively low AS-POSS content, which characterizes this mixture as a polymer nanocomposite system. ©2006 Wiley Periodicals, Inc. *J Polym Sci Part B: Polym Phys* 44: 673–686, 2006

**Keywords:** 2D-FTIR; hydrogen bonding; nanocomposite; POSS

## INTRODUCTION

Incorporating nanoparticles into polymer matrices to enhance their properties has attracted enormous interest in recent years because of the potential to create candidate materials that bridge the gap between polymers and nanoparticles. In particular, the use of polyhedral oligomeric silsesquioxanes (POSS) derivatives is one suitable approach because they embody an inorganic–organic hybrid architecture comprising a

well-defined inorganic framework composed of silicon and oxygen ( $\text{SiO}_{1.5}$ )<sub>x</sub> and organic substituents containing nonreactive or reactive functionalities. By designing the functionality of the organic substituents, it is possible to create octafunctional or monofunctional macromonomers to fit a desired application. Therefore, these nanostructured compounds can be incorporated readily through copolymerization into such polymers as polysiloxane,<sup>1</sup> poly(methyl methacrylate),<sup>2,3</sup> poly(styrene),<sup>4</sup> epoxy,<sup>5</sup> polyurethane,<sup>6</sup> polyimide,<sup>7</sup> and polynorbornene.<sup>8</sup>

The physical properties of polymer/POSS nanocomposites are strongly influenced by the miscibility between the host polymer and the POSS moiety. Random copolymerization of the organic

Correspondence to: S.-W. Kuo (E-mail: kuosw@mail.nctu.edu.tw)

*Journal of Polymer Science: Part B: Polymer Physics*, Vol. 44, 673–686 (2006)  
©2006 Wiley Periodicals, Inc.

functional groups of the POSS derivative is one approach to improving the miscibility. Therefore, in a previous study,<sup>9</sup> we synthesized a series of poly(vinylphenol-co-vinylpyrrolidone-co-POSS) (PVPh-co-PVP-co-POSS) copolymers that exhibit a significant glass-transition temperature increase relative to the corresponding nonPOSS PVPh-co-PVP copolymers because of the strong hydrogen bonds that exist between the PVPh and POSS units. The synthesis of a random copolymer is generally more complicated and time-consuming than is preparing a physical blend; thus, polymer blending is seen as a more convenient method of preparing polymer/POSS nanocomposites. Because the combined entropy contribution to the free energy of mixing two polymers is negligibly small, specific intermolecular interactions are generally required to enhance the miscibility of polymer blends. To improve the properties and miscibility of hybrid materials, it is necessary to ensure that favorable, specific interactions exist between these components, such as hydrogen bonding,<sup>10</sup> dipole-dipole, and acid-base interactions.

In a previous study,<sup>11</sup> we demonstrated that simple blending of POSS derivatives containing nonreactive or inert diluent functional groups (in that case, octaisobutyl-POSS) with phenolic resin provide unsatisfactory results because of poor miscibility. The interassociation equilibrium constant between the phenolic hydroxyl group and the octaisobutyl-POSS siloxane group (38.6) is lower than the self-association equilibrium constant of pure phenolic (52.3), based on the Painter-Coleman association model<sup>10</sup> (PCAM). This result indicates that this POSS derivative tends to be only partially miscible with phenolic in the phenolic/POSS hybrid because of the poor degree of interaction between the phenolic resin and the octaisobutyl-POSS. Functionalization of POSS such that it displays pendent hydrogen-bond-acceptor groups is expected to improve the miscibility with phenolic resin. Functionalization of  $Q_8M_8^H$  [ $HSiMe_2OSiO_{1.5}$ ]<sub>8</sub> can be achieved by hydrosilylation of its Si-H groups onto acetoxystyrene in the presence of a platinum catalyst to form AS-POSS. Previously, we used infrared and solid-state NMR spectroscopy to thoroughly investigate the hydrogen bonding interactions between the carbonyl groups of poly(acetoxystyrene) (PAS) and the hydroxyl groups of phenolic resin.<sup>12</sup> We found that the interassociation equilibrium constant for the phenolic/PAS blend (64.6) is higher than the self-association equilibrium constant of

pure phenolic (52.3), which implies that the tendency for hydrogen bonding between the phenolic resin and PAS dominates over the self-association (intramolecular hydrogen bonding) of the phenolic resin in the mixture.

Observing the carbonyl, hydroxyl, and siloxane vibrations by infrared (FTIR) spectroscopy is an excellent tool for detecting intermolecular polymeric interactions.<sup>13</sup> This tool can be used to study the mechanism—both qualitatively and quantitatively—of interpolymer miscibility through the formation of different types of hydrogen bonds. In addition, the generalized two-dimensional (2D) IR correlation spectroscopy<sup>14–19</sup> has been applied widely in polymer science in recent years. In 2D IR, a spectrum is obtained as a function of two independent wavenumber axes, and peaks located on the spectral plane. This novel method monitors spectral fluctuations as a function of time, temperature, pressure, and composition and allows the specific interactions that exist between polymer chains to be identified. 2D IR correlation spectroscopy can identify different intra- and intermolecular interacting sites through the monitoring of selected bands from the one-dimensional vibration spectrum. In this study, we used generalized 2D IR correlation spectroscopy to explore the hydrogen bonding interactions present in blends of AS-POSS and phenolic resin.

The interassociation equilibrium constant between the phenolic hydroxyl groups and the POSS siloxane groups cannot be quantified directly through IR spectroscopic analysis in this binary blend because no carbonyl groups are available to measure the fraction of groups that are hydrogen bonded. The siloxane stretching mode near 1100–1200  $cm^{-1}$ , which presents signals for both the free and hydrogen-bonded siloxane absorptions, is a highly coupled mode that is conformationally sensitive but cannot be decomposed readily into two peaks. In a previous study,<sup>11</sup> we calculated the interassociation equilibrium constant ( $K_A$ ) between the hydroxyl groups of phenolic resin and the siloxane group of octaisobutyl-POSS by using the classical Coggesthall and Saier (C and S)<sup>20</sup> methodology. The interassociation equilibrium constant obtained from low molecular weight compounds, however, is not exactly the same as that calculated for a true polymer blend because intramolecular screening and functional group accessibility affect the miscibility of a polymer blend.<sup>21</sup> Fortunately, in our previous study,<sup>11</sup> octaisobutyl-POSS was the low-molecular-weight compound and, thus, this calculation can be

considered to provide the true interassociation equilibrium constant for the interactions between the phenolic hydroxyl groups and the POSS siloxane groups. To recheck the interassociation equilibrium constant between the phenolic hydroxyl groups and the POSS siloxane groups in this present study, we determined the value of  $K_A$  indirectly from a least-squares fitting procedure of the experimental fraction of hydrogen-bonded carbonyl groups of AS-POSS in this binary blend. We have found a good correlation between these two methods for determining the interassociation equilibrium constant of the hydroxyl–siloxane interactions.

## EXPERIMENTAL

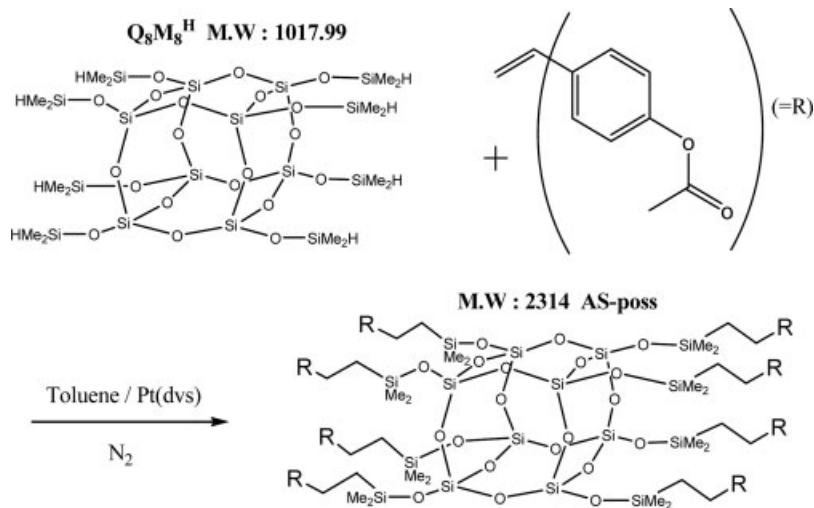
### Materials

The phenolic used in this study was synthesized through a condensation reaction with sulfuric acid to give average weights of  $M_n = 500$  and  $M_w = 1200$ .  $Q_8M_8^H$  was purchased from Hybrid Plas-

tics Co. Platinum divinyltetramethyldisiloxane complex, Pt(dvs), and acetoxystyrene were obtained from Aldrich Chemical Co. Inc. Octa(acetoxystyryl)octasilsesquioxane (AS-POSS) was synthesized according to the following method.

### Synthesis of Octa(acetoxystyryl)octasilsesquioxane (AS-POSS)

$Q_8M_8^H$  (2.00 g, 1.96 mmol) was dissolved in toluene (20 mL) in a 100-mL Schlenk flask, equipped with a reflux condenser and a magnetic stirrer, and then 4-acetoxystyrene (3.2 g, 19.6 mmol) was added. Pt(dvs) (2 mM solution, 0.2 mL) was added through a syringe. The reaction mixture was heated to 80 °C under nitrogen. The reaction was complete within 4 h. The toluene was evaporated under reduced pressure, and the residue was dried in a vacuum oven at 80 °C for 24 h to give AS-POSS (3.17 g, 93%). AS-POSS is a colorless, viscous liquid that is soluble in THF,  $CHCl_3$ , and acetone. The chemical structure and scheme for the synthesis of AS-POSS are shown here:



### Blend Preparation

Blends of phenolic/AS-POSS of various compositions were prepared by solution blending. A THF solution containing 5 wt % of the mixture was stirred for 6–8 h and then the solvent was evaporated slowly at room temperature over 1 day. To ensure total elimination of solvent, the powder of the blend obtained was dried in a vacuum oven at 60 °C for 2 days.

### Characterization

#### Nuclear Magnetic Resonance ( $^1H$ NMR) Spectroscopy

$^1H$  NMR spectra were recorded on a Varian Unity Inova 500 FT NMR spectrometer operating at 500 MHz, using  $CDCl_3$  as the solvent; chemical shifts are reported in parts per million (ppm).

### Fourier Transform Infrared (FTIR) Spectroscopy

Infrared spectroscopic measurements were recorded on a Nicolet Avatar 320 FTIR spectrophotometer; 32 scans were collected with a spectral resolution of  $1\text{ cm}^{-1}$ . Infrared spectra of polymer blend films were obtained through the conventional NaCl disk method. All sample preparations were performed under a continuous flow of nitrogen to minimize sample oxidation or degradation. Samples were prepared by casting a THF solution directly onto a NaCl disk, which was dried under conditions similar to those used in the bulk preparation.

2D IR correlation analysis was conducted using Vector 3D software (Bruker Instrument Co.). All of the spectra were normalized before being subjected to 2D correlation analyses. All of the spectra subjected to the 2D correlation analyses were normalized and classified into two sets: A and B. The spectra in set A are, in order, pure phenolic, phenolic/AS-POSS = 5/95, phenolic/AS-POSS = 10/90, and phenolic/AS-POSS = 20/80. Those in set B are, in order, phenolic/AS-POSS = 30/70, phenolic/AS-POSS = 40/60, phenolic/AS-POSS = 60/40, and pure AS-POSS. Shaded areas indicate regions of negative intensity of auto-peaks or crosspeaks in the 2D correlation spectrum; unshaded areas indicate positive-intensity regions. Synchronous 2D spectra were used to study the specific interactions between phenolic and AS-POSS in the blends.

### Differential Scanning Calorimetry (DSC)

Thermal analysis was performed using a DuPont DSC-9000 differential scanning calorimeter at a scan rate of  $20\text{ }^{\circ}\text{C}/\text{min}$  over a temperature range from  $-50$  to  $150\text{ }^{\circ}\text{C}$ . Temperature and energy calibrations were undertaken using indium. Approximately 5–10 mg of each blend was weighed and sealed in an aluminum pan. This sample was quickly cooled to  $-50\text{ }^{\circ}\text{C}$  from the melt of the first scan and then it was scanned between  $-50$  and  $150\text{ }^{\circ}\text{C}$  at  $20\text{ }^{\circ}\text{C}/\text{min}$ . The glass-transition temperature was obtained at the midpoint of the specific heat increment.

## RESULTS AND DISCUSSION

### AS-POSS Analyses

Figure 1(a) presents the FTIR spectra of  $\text{Q}_8\text{M}_8^{\text{H}}$ , acetoxystyrene, and the final hydrosilylation product, AS-POSS. The strong absorption peak at  $1100$

$\text{cm}^{-1}$  for both  $\text{Q}_8\text{M}_8^{\text{H}}$  and AS-POSS represents the vibrations of the siloxane Si—O—Si groups and is a general feature of POSS derivatives. The characteristic stretching vibrations of the vinyl ( $\text{ArCH}=\text{CH}_2$ ) and Si—H groups appear as peaks at  $1650$  and  $2200\text{ cm}^{-1}$ , respectively. In AS-POSS, these peaks have disappeared completely, indicating that complete reaction was achieved. Furthermore, the peak for the carbonyl groups of the acetoxystyrene ( $1765\text{ cm}^{-1}$ ) remained in AS-POSS, which provides evidence for the successful attachment of the acetoxystyrene units to the POSS core. Figure 1(b) displays the corresponding  $^1\text{H}$  NMR spectra of AS-POSS. Clearly, the peaks for the vinyl (ca. 5.8 ppm) and Si—H protons (4.7 ppm) have disappeared in the spectrum of AC-POSS, which supports the complete reaction. The spectrum in Figure 1(b) indicates that the vinyl groups of acetoxystyrene underwent hydrosilylation of the Si—H bonds of  $\text{Q}_8\text{M}_8^{\text{H}}$  in both  $\alpha$  and  $\beta$  configurations, which is a mixture of these two orientation exists. From the integrated areas of the two types of methyl groups attached to the Si atoms, we estimate that  $\alpha$ -carbon atom attachment was three times as prevalent as  $\beta$ -carbon atom attachment.

### 1D IR Spectral Analyses of Phenolic/AS-POSS Nanocomposites

In a previous study,<sup>11</sup> we used 1D and 2D FTIR spectra to discuss in detail the hydrogen bonding interactions that exist between the phenolic hydroxyl groups and the POSS siloxane groups. In addition, we have also studied<sup>22</sup> the weak specific hydrogen bonding interactions between the carbonyl groups of PAS and the methylene units of PEO. In this study, we synthesized an acetoxystyrene (AS)-grafted POSS (AS-POSS) to investigate the specific interactions between phenolic and AS-POSS. Figure 2 displays infrared spectra of phenolic/AS-POSS blends in different compositions and Table 1 lists detailed peak assignments for phenolic and AS-POSS.

Figure 3(a) presents scaled infrared spectra ( $2700$ – $4000\text{ cm}^{-1}$ ) recorded at room temperature from pure phenolic and various phenolic/AS-POSS nanocomposites. The pure phenolic polymer exhibits two bands in the hydroxyl stretching region of the infrared spectrum. We attributed the very broadband centered at  $3350\text{ cm}^{-1}$  to the wide distribution of hydrogen-bonded hydroxyl groups, while a narrower shoulder band at  $3525\text{ cm}^{-1}$  represents the free hydroxyl groups. Figure 3(a) indicates clearly that the intensity of the free

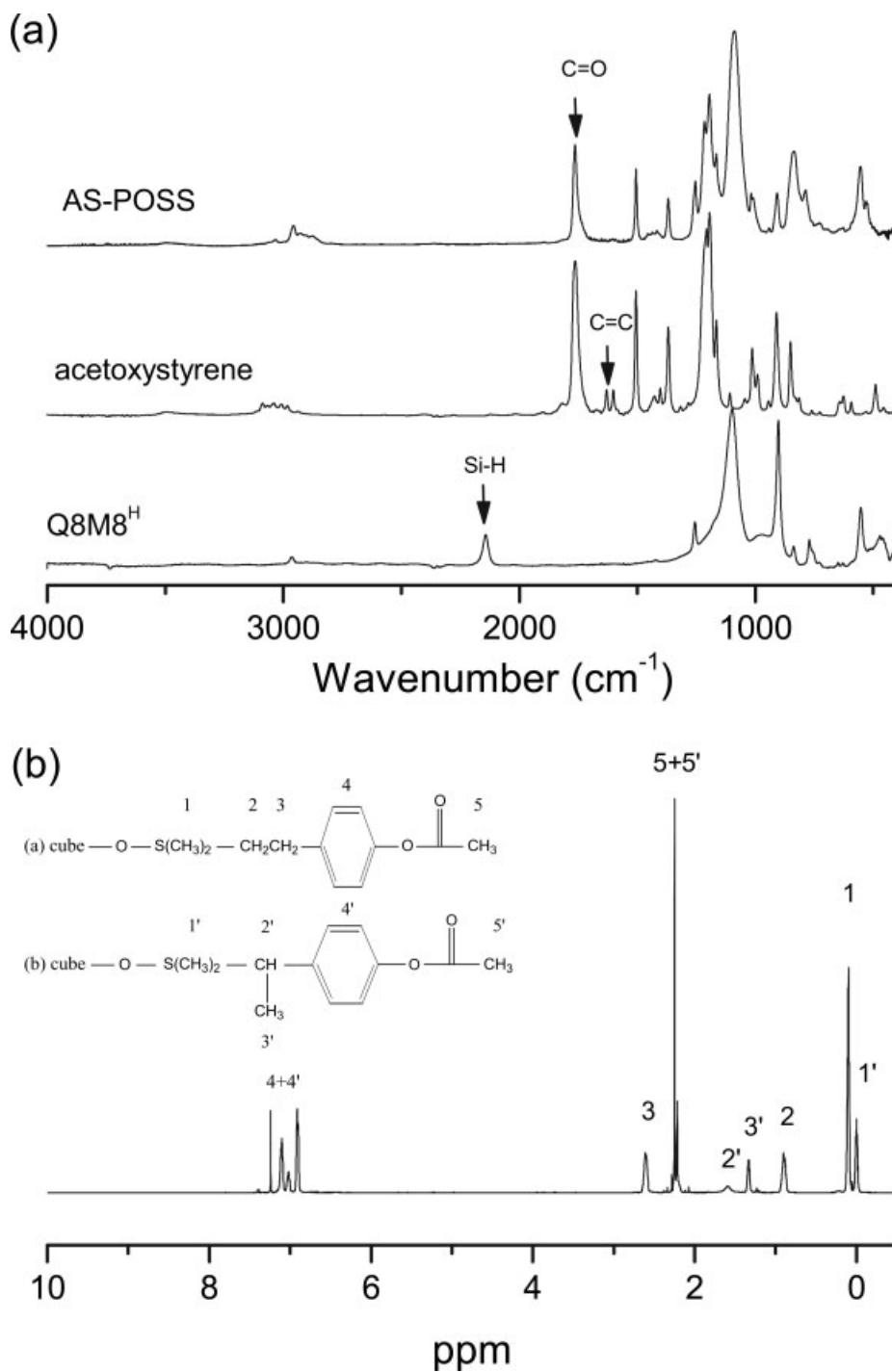


**Figure 1.** (a) IR spectra recorded at room temperature for Q<sub>8</sub>M<sub>8</sub><sup>H</sup>, acetoxystyrene, and AS-POSS and (b) the <sup>1</sup>H NMR spectrum of AS-POSS.

hydroxyl absorption (3525 cm<sup>-1</sup>) decreases gradually as the AS-POSS content of the blend increases from 5 to 90 wt %. The band for the hydrogen-bonded hydroxyl units in the phenolic tends to shift to higher frequency (toward 3465 cm<sup>-1</sup>) upon increasing the AS-POSS content. This

change is due to the switch from hydroxyl–hydroxyl interactions to the formation of hydroxyl–carbonyl and/or hydroxyl–siloxane hydrogen bonds.

Figure 3(b) displays the infrared spectra (1680–1820 cm<sup>-1</sup>) measured at room temperature for various phenolic/AS-POSS blend composi-

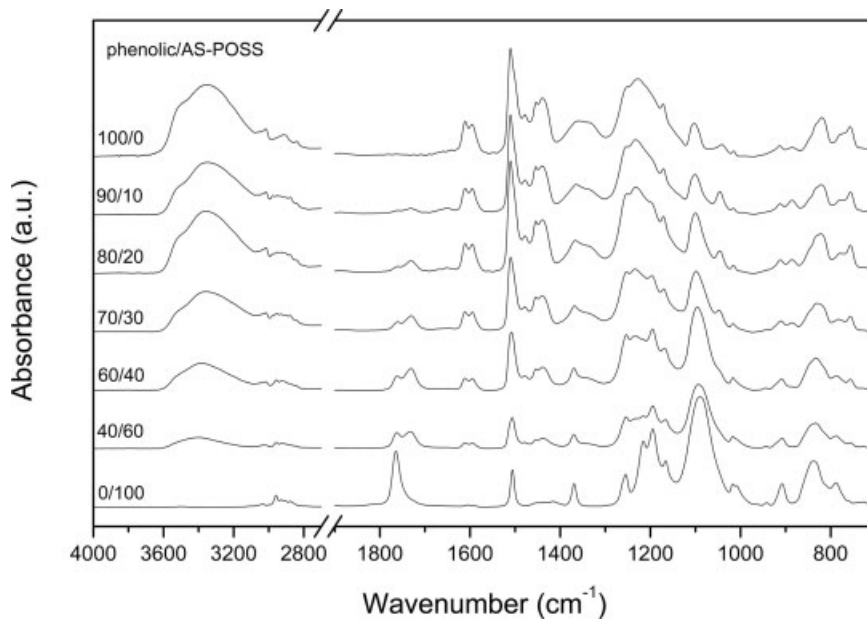


**Figure 2.** Infrared spectra recorded at room temperature for phenolic/AS-POSS blends of various compositions.

**Table 1.** Frequency and Peak Assignments of the FTIR Spectral Bands of Phenolic and AS-POSS

Phenolic ( $\text{cm}^{-1}$ )	AS-POSS ( $\text{cm}^{-1}$ )	Assignments
3525		Free OH-stretching
3350		Hydrogen-bonded OH-stretching
	3037	Benzene ring CH stretching
3016		Benzene ring CH stretching
	2957	$\text{CH}_2$ stretching
2916		$\text{CH}_2$ stretching
2841		$\text{CH}_2$ stretching
	1763	Free C=O stretching
1611,1595		C–C stretching of ring in plane
	1603	C–C stretching of ring in plane
1510		Phenyl–OH stretching
	1505	Phenyl–O– stretching
1478,1439		Asymmetric $\text{CH}_2$ stretching
	1455,1421	Asymmetric $\text{CH}_2$ stretching
	1368	Symmetric carboxylate stretching
1357		COH bending
1223		phenyl–OH stretching
	1230	Si– $\text{CH}_2$ stretching
	1215	Acetate stretching
	1193	Acetate asymmetric stretching
1102		C–O stretching
	1087	Si–O–Si Stretching
	1015	C–O stretching
	911	$\text{CH}_2$ out of line bending
	846	$\text{CH}_2$ out of line bending

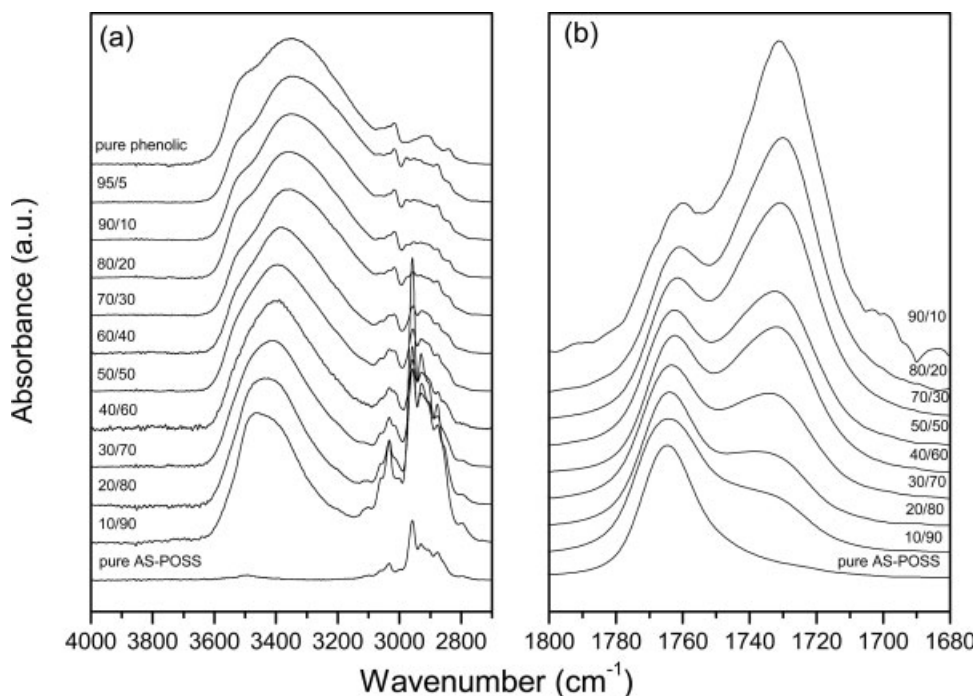


**Figure 3.** Infrared spectra recorded at room temperature for phenolic/AS-POSS blends and displaying the (a) hydroxyl stretching and (b) carbonyl stretching regions.

tions. The carbonyl stretching frequency is split into two bands at 1763 and 1735  $\text{cm}^{-1}$ , which corresponds to the free and hydrogen-bonded carbonyl groups, respectively. The band can be readily decomposed into two Gaussian peaks that corresponds to the areas of the hydrogen-bonded carbonyl (1735  $\text{cm}^{-1}$ ) and free carbonyl (1763  $\text{cm}^{-1}$ ) peaks, as indicated in Figure 4. To obtain the fraction of the hydrogen-bonded carbonyl units, we required the absorptivity ratio for the contributions of the hydrogen-bonded and free carbonyl units. We have employed a value for  $\alpha_{\text{HB}}/\alpha_{\text{F}}$  of 1.5, as calculated previously by Coleman et al.<sup>10</sup> Table 2 summarizes the fractions of hydrogen-bonded carbonyl groups obtained through curve fitting. As expected, this value rises upon increasing the phenolic content.

### 2D IR Spectral Analyses of Phenolic/AS-POSS Nanocomposites

In the studies of the 1D-IR spectra earlier, we found that the signal of the hydroxyl groups of phenolic shifts dramatically higher (or lower) upon adding AS-POSS, and we propose that this change is due to the switch from hydroxyl-hydroxyl interactions to hydroxyl-carbonyl and/or hydroxyl-siloxane hydrogen bonds. In this sec-

tion, we describe how we used 2D-IR spectra to investigate these types of hydrogen bonds.

Figure 5 displays synchronous 2D correlation maps (900 to 1300  $\text{cm}^{-1}$ ) of blends and indicates that strong auto and cross peaks exist at wavenumbers between 1100 and 1250  $\text{cm}^{-1}$ . The absorption bands of the POSS derivative that appear in the spectral range from 1250 to 1000  $\text{cm}^{-1}$  are those at 1100 and 1230  $\text{cm}^{-1}$ , which correspond to siloxane Si—O—Si and Si—CH<sub>2</sub> stretching vibrations, respectively; for phenolic, only one appears (at 1223  $\text{cm}^{-1}$ ; it is due to phenyl—OH stretching vibrations) based on Table 1. The two positive cross peaks in Figure 2 indicate that the hydrogen bonding interactions occur between the siloxane groups of AS-POSS (1100  $\text{cm}^{-1}$ ) and the phenyl—OH groups of phenolic (1223  $\text{cm}^{-1}$ ), which are similar to those observed for phenolic/isobutyl-POSS blends.<sup>11</sup>

Figure 6 also displays the synchronous 2D correlation maps (1500–1800  $\text{cm}^{-1}$ ) of blends. The three strong auto peaks and two pairs of cross peaks near the 1510, 1750, and 1600  $\text{cm}^{-1}$  regions correspond to vibrations of the phenol—OH, carbonyl, and aromatic groups, respectively. In the 1750  $\text{cm}^{-1}$  region, we observe two auto peaks clearly at 1735 and 1763  $\text{cm}^{-1}$ ; they correspond to the free carbonyl groups of AS-POSS and those

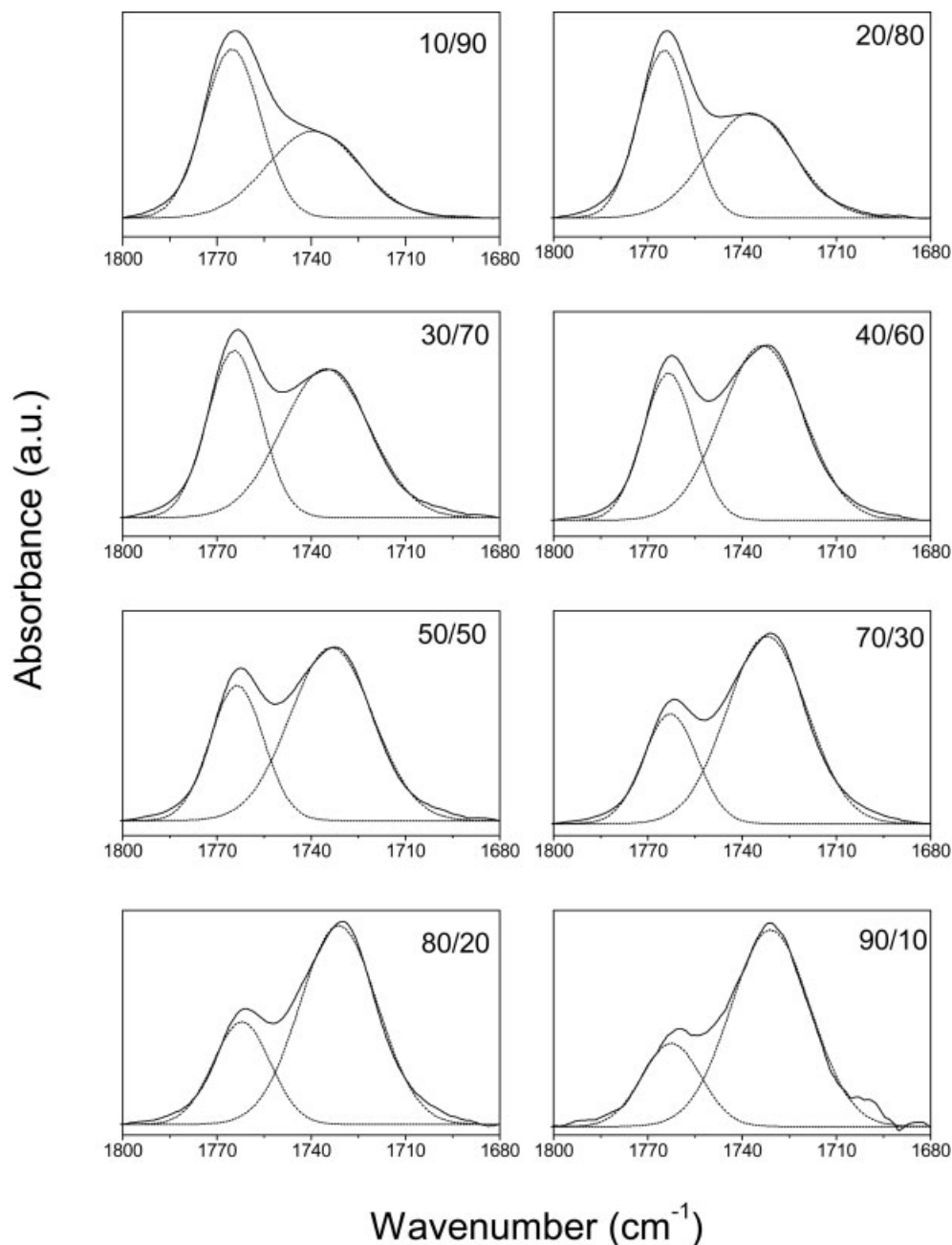


**Figure 4.** Deconstructed models of the carbonyl stretching bands [in Fig. 3(b)] with respect to the weight percentages of the phenolic/AS-POSS blends at various compositions.

that are hydrogen bonded to the phenolic hydroxyl groups, respectively. In the  $1600\text{ cm}^{-1}$  region, we observe two auto-peaks at  $1590$  and  $1610\text{ cm}^{-1}$  that correspond to the phenyl groups in both phenolic and AS-POSS. Figure 6 indicates clearly that hydrogen bonding interactions do indeed exist between the carbonyl groups of AS-POSS ( $1763\text{ cm}^{-1}$ ) and the phenyl—OH groups of the phenolic resin ( $1510\text{ cm}^{-1}$ ).

#### Hydroxyl–Siloxane Inter-Association Equilibrium Constant Determined through PCAM Analysis

According to the PCAM, the interassociation equilibrium constant between a noncarbonyl group component and a hydrogen bond-donating component can be calculated using the classical Coggesthall and Saier method.<sup>20</sup> To recheck the interassociation equilibrium constant between the phenolic hydroxyl groups and the POSS silox-



**Table 2.** Curve Fitting of the Area Fractions of the Carbonyl Stretching Bands in the FTIR Spectra of Phenolic/AS-Poss Blends Recorded at Room Temperature

Phenolic/ AS-POSS (Wt Ratio)	Free C=O			H-Bonding C=O			$f_b^a$
	$\nu$ ( $\text{cm}^{-1}$ )	$W_{1/2}$ ( $\text{cm}^{-1}$ )	$A_f$ (%)	$\nu$ ( $\text{cm}^{-1}$ )	$W_{1/2}$ ( $\text{cm}^{-1}$ )	$A_b$ (%)	
0/100	1763	23	100	—	—	—	—
10/90	1765	18	52.6	1739	30	47.4	0.375
20/80	1765	17	41.5	1737	28	58.5	0.484
30/70	1764	17	36.1	1736	28	63.9	0.541
40/60	1764	16	32.6	1734	26	67.4	0.580
50/50	1763	17	29.9	1734	26	70.1	0.610
70/30	1763	17	25.6	1732	26	74.4	0.660
80/20	1762	18	23.3	1731	25	76.7	0.688
90/10	1762	18	22.1	1731	25	77.9	0.701

<sup>a</sup>  $f_b$ , fraction of hydrogen bonding interaction.  
 $\nu$ , wavenumber;  $W_{1/2}$ , half width.

ane groups in this present study, we determined the value of  $K_A$  indirectly from a least-squares fitting procedure of the experimental fraction of hydrogen-bonded carbonyl groups of AS-POSS in this binary blend. Figure 7 displays plots of the experimental data and theoretically predicted

curves as a function of the composition at room temperature. The results demonstrate that PCAM has the ability to predict the degree of hydrogen bonding on the carbonyl group. Figure 7 indicates that the experimental values are generally lower than the predicted values when

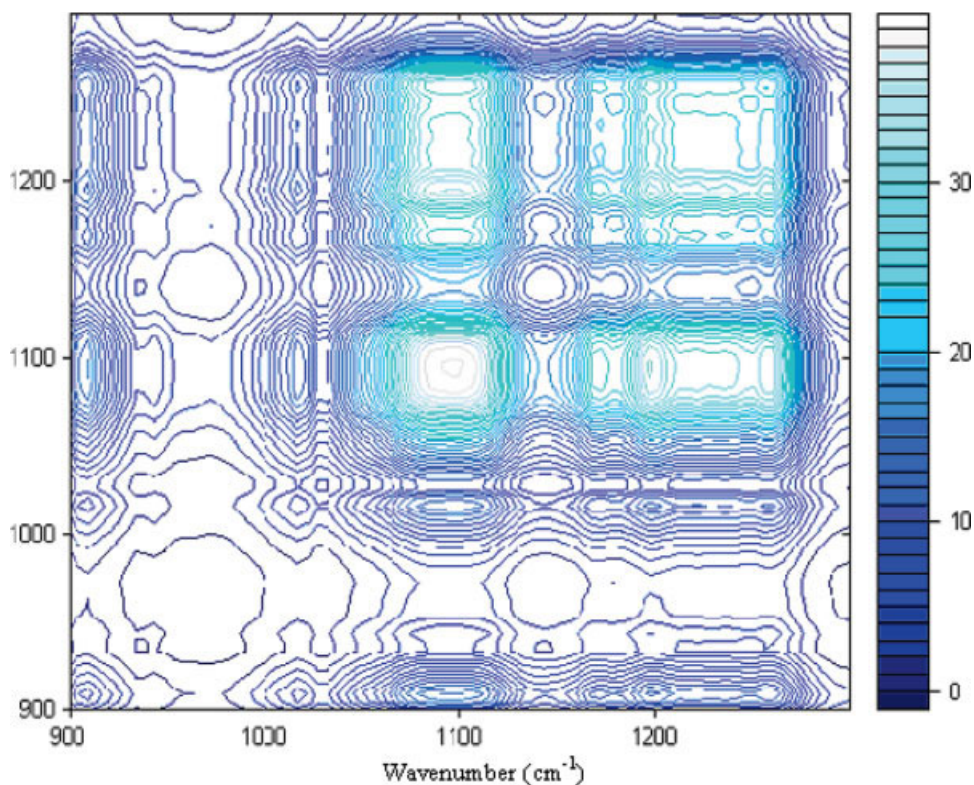


**Figure 5.** The synchronous 2D correlation map of set A in the 900–1300  $\text{cm}^{-1}$  region. (The y-axis is wavenumber ( $\text{cm}^{-1}$ )). [Color figure can be viewed in the online issue, which is available at [www.interscience.wiley.com](http://www.interscience.wiley.com).]

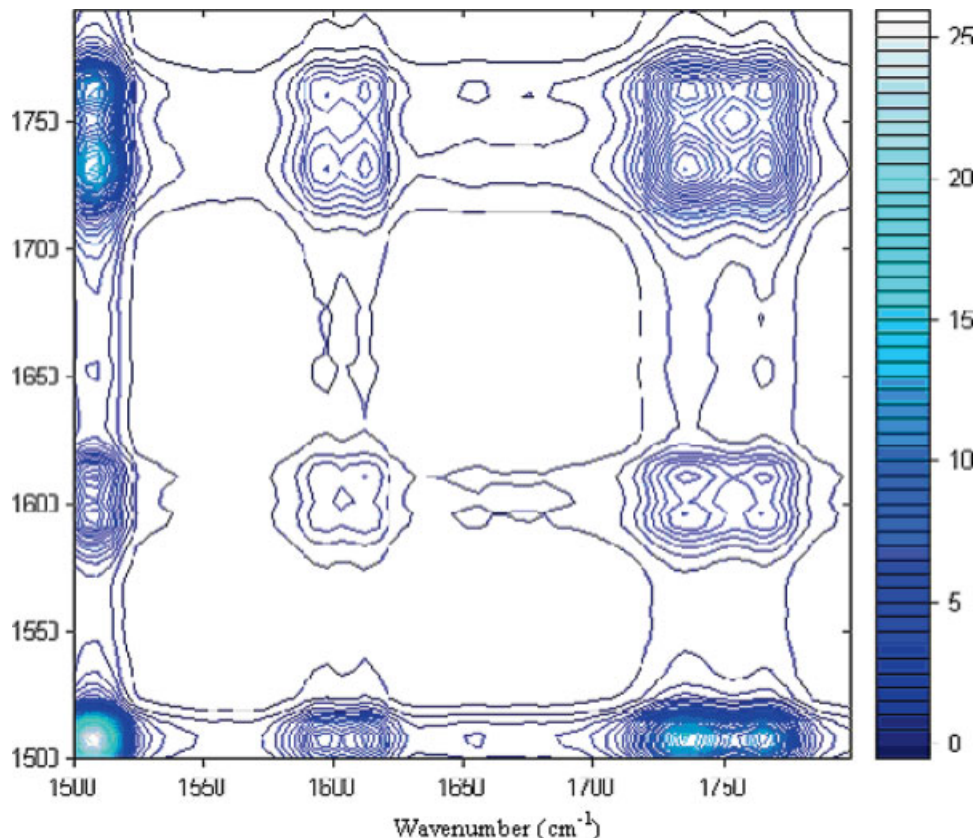


**Figure 6.** The synchronous 2D correlation map of set A in the 1500–1800  $\text{cm}^{-1}$  region. (The y-axis is wavenumber ( $\text{cm}^{-1}$ )). [Color figure can be viewed in the online issue, which is available at [www.interscience.wiley.com](http://www.interscience.wiley.com).]

using the value of  $K_A$  of 64.6 obtained from phenolic/PAS blends. This result also indicates that the hydroxyl groups of phenolic not only interact with the carbonyl groups of the acetoxystyrene units but also with the siloxane groups of the POSS core, which is consistent with our results from a previous study.<sup>11</sup> In other words, the AS carbonyl groups compete with the siloxane groups of the POSS core in forming hydrogen bonds with the hydroxyl groups of the phenolic resin. We employed a numerical method to determine the value of  $K_A$  of the phenolic/AS-POSS blend, according to the PCAM, based on the fraction of hydrogen-bonded carbonyl groups. The approximate equations<sup>10</sup> are as follows:

$$\Phi_B = \Phi_{B1}\Gamma_2 \left[ 1 + \frac{K_A\Phi_{A1}}{r_A} \right] \quad (1)$$

$$\Phi_A = \Phi_{A1}[1 + K_A\Phi_{B1}\Gamma_1] \quad (2)$$

where

$$\Gamma_1 = \left( 1 - \frac{K_2}{K_B} \right) + \frac{K_2}{K_B} \left( \frac{1}{(1 - K_B\Phi_{B1})} \right) \quad (3)$$

$$\Gamma_2 = \left( 1 - \frac{K_2}{K_B} \right) + \frac{K_2}{K_B} \left( \frac{1}{(1 - K_B\Phi_{B1})^2} \right) \quad (4)$$

and  $\phi_A$  and  $\phi_B$  denote the volume fractions of the nonself-associated species A (AS-POSS) and the self-associating species B (phenolic), respectively;  $\phi_{A1}$  and  $\phi_{B1}$  are the corresponding volume fractions of the isolated AS-POSS and phenolic segments, respectively;  $r$  is the ratio of molar volume,  $V_A/V_B$ . The self-association equilibrium constants,  $K_B$  and  $K_2$ , describe the formation of multimers and dimers, respectively. Finally,  $K_A$  is the equilibrium constant describing the association of A with B. The values of  $K_B$  and  $K_2$  of pure phenolic at 25 °C are 23.3 and 52.3, respectively.<sup>11</sup> To calculate the values of the interassociation constants  $K_A$ , we used a least-squares method that we had described previously.<sup>12</sup> Table 3 lists all of the parameters required by the Painter–

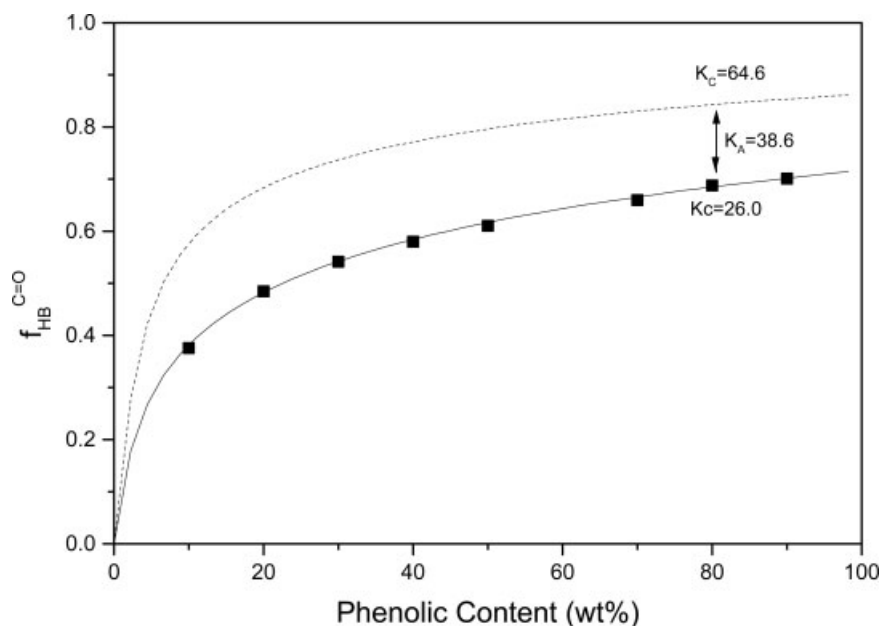


**Figure 7.** Fraction of hydrogen-bonded carbonyl groups plotted with respect to the composition of the blend: (■) FT-IR spectroscopic data, (—) theoretical values from phenolic/PAS blends ( $K_A = 64.6$ ), and (---) theoretical values from phenolic/AS-POSS blends ( $K_A = 26.0$ ) calculated at 25 °C.

Coleman association model to estimate the thermodynamic properties for this phenolic/AS-POSS blend. We obtained an interassociation equilibrium constant of 26.0 for the phenolic/AS-POSS blend. It is difficult to exactly separate the segment of AS and POSS because of the chemical bond between these two segments, and so we assume that the molar volume of AS and POSS segment is the same (ca. 1000 mL/mol). The value of  $K_A$ , however, for the phenolic/PAS blend is 64.6, which implies that the value of  $K_A$  between the hydroxyl group of phenolic and the siloxane group of POSS is equal to 38.6 (*i.e.* 64.6 – 26.0 = 38.6), which is entirely consistent with the value reported previously based on classical Coggeshall and Saier (C and S) methodology. Therefore, there is a good correlation between these two different methods when determining the values of the interassociation equilibrium constants for hydroxyl–siloxane interactions.

### Thermal Analyses

In general, DSC analysis is one of the most convenient methods for determining the miscibility of blend systems. DSC can determine whether one or two values exist for  $T_g$ : a single value of  $T_g$  is the most conventionally used criterion for

establishing the miscibility of polymer blends; an immiscible polymer blend exhibits more than one value of  $T_g$ . A single compositionally dependent glass transition indicates full miscibility with dimensions of the order of 20–40 nm. The miscibilities of most polymer/nanoparticle blend systems have not been studied using DSC analyses, however, because most of these nanoparticles

**Table 3.** Self- and Inter-Association Equilibrium Constants and Other Thermodynamic Parameters of Phenolic/AS-Poss Blends at 25 °C

Polymer	$V$	$M_w$	Equilibrium Constant		
			$K_2$	$K_B$	$K_A$
Phenolic <sup>a</sup>	84	105	23.3	52.3	
PAS <sup>b</sup>	128.6	162.2			64.6
8-Isobutyl POSS <sup>c</sup>	778.6	872.2			38.6
AS-POSS	2058.6	2314.6			26.0

<sup>a</sup> reference <sup>11</sup>.

<sup>b</sup> reference <sup>12</sup>.

<sup>c</sup> reference <sup>11</sup>.

$V$ , molar volume (ml/mol);  $M_w$ , molecular weight (g/mol);  $K_2$ , dimer self-association equilibrium constant;  $K_B$ , multimer self-association equilibrium constant;  $K_A$ , inter-association equilibrium constant.

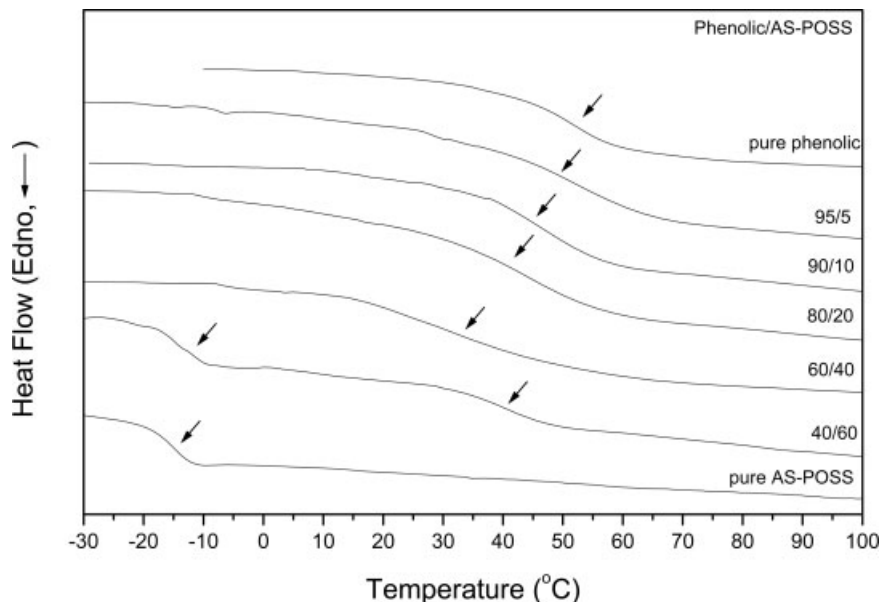


**Figure 8.** DSC scans of phenolic/AS-POSS blends having different compositions.

have been inorganic materials that do not display a glass transition at relatively lower temperatures ( $<400\text{ }^{\circ}\text{C}$ ). Fortunately, we obtained conventional second-run DSC thermograms of the phenolic/AS-POSS blends at various compositions, as presented in Figure 8. The glass-transition temperatures of the pure components used in this study, phenolic and AS-POSS, are  $53$  and  $-15\text{ }^{\circ}\text{C}$ , respectively. Interestingly, even though the molar masses of pure phenolic and AS-POSS are only  $1200$  and  $2305\text{ g/mol}$ , they display single- $T_g$  behavior at  $52.5$  and  $-15\text{ }^{\circ}\text{C}$ , respectively, during the second heating scan. We must emphasize that phenolic resin contains a high density of hydroxyl groups and that hydrogen bonding serves as a physical crosslink to increase its glass-transition temperature. In addition, phenolic resin possesses a higher value of  $T_g$  than do other materials that have similar molecular weights because of its high density of hydrogen bonds. Pure AS-POSS can be considered as an oligomer of the siloxane and acetoxystyrene. We also rechecked the thermal analysis of  $Q_gM_g^H$  by DSC. We observed no glass transition, which indicates that the glass-transition temperature of AS-POSS is a result of the presence of the acetoxystyrene segments.

We observed clearly that a single value of  $T_g$  existed for those blends having relatively low AS-POSS contents ( $<40\text{ wt }%$ ) and that the value of  $T_g$  decreased upon increasing the AS content. In addition, the  $T_g$  breadth also increased upon

increasing the AS content (from  $12\text{ }^{\circ}\text{C}$  for pure phenolic to  $34\text{ }^{\circ}\text{C}$  for phenolic/AS-POSS =  $60/40$ ), which implies that the homogeneity decreases at the molecular scale of the blend system upon an increase in the AS-POSS content. At a higher AS-POSS content ( $60\text{ wt }%$ ), however, we found two values of  $T_g$  for those phenolic/AS-POSS blends, indicating their immiscibility. According to the infrared spectral analyses, the fraction of hydrogen-bonded carbonyl groups decreased upon increasing the AS-POSS content; thus, phase separation may occur at higher AS-POSS content because the lower fraction of hydrogen bonding interactions does not overcome the strong ability of AS-POSS nanoparticles to aggregate. This result is entirely likely because we found in this study that the interassociation equilibrium constant ( $K_A = 64.6$ ) for the interaction between the carbonyl groups of AS-POSS and the hydroxyl groups of phenolic is not significantly higher than the self-association equilibrium constant of pure phenolic ( $K_B = 52.3$ ). Therefore, at a higher AS-POSS content, the ability of AS-POSS nanoparticles to aggregate immiscibly dominates over the benefits of hydrogen bonding. In summary, we have demonstrated that the miscibility behavior in this phenolic/AS-POSS blend is dependent on the extent of the hydrogen bonding interactions, while the immiscible aggregation ability of AS-POSS nanoparticles, which is similar to that of many polymer nanocomposite systems, decreases upon increasing the nanoparticle's content.<sup>23</sup>

If we take into account, only the results obtained at relatively low AS-POSS contents (<40 wt %), these compositions display miscibility and variable glass-transition temperatures as a function of the composition of the blend, as indicated in Figure 9. A number of equations have been designed to predict the variations in the glass-transition temperatures of miscible blends in relation to their composition. The most widely used equation is the Kwei equation,<sup>24</sup> which predicts the glass-transition temperature of a miscible blend featuring hydrogen bonding interactions as a function of its composition:

$$T_g = \frac{W_1 T_{g1} + kW_2 T_{g2}}{W_1 + kW_2} + qW_1 W_2 \quad (5)$$

where  $W_1$  and  $W_2$  denote the weight fractions of the compositions,  $T_{g1}$  and  $T_{g2}$  represent the corresponding glass-transition temperatures of the blend's components, and  $k$  and  $q$  are fitting constants. Figure 9 displays plots of the values of  $T_g$  of the blends *versus* their compositions; clearly, the linear and Fox equations do not fit the exper-

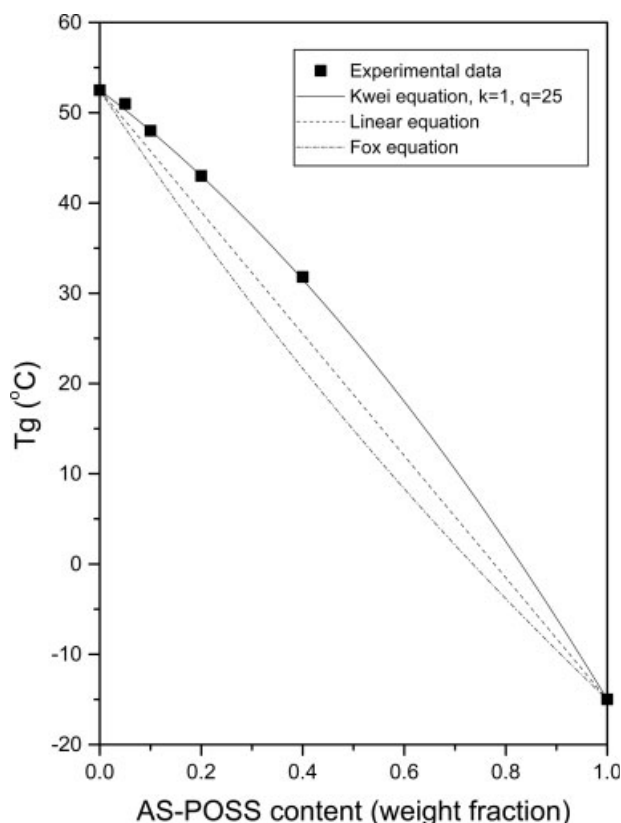


**Figure 9.** Plots of  $T_g$  versus composition based on the experimental data and the linear, Fox, and Kwei equations.

imental data well. The Kwei equation, however, correlates well with the experimental data. On the basis of the nonlinear least-squares best fit of this data, we obtained  $k = 1$  and  $q = 25$ ;  $q$  is a parameter that corresponds to the strength of the hydrogen bonds in the blend and reflects the balance between the breaking of any self-association and the formation of the interassociation hydrogen bonds. Compared with the phenolic/PAS blend system ( $k = 1$ ,  $q = -245$ ),<sup>12</sup> the phenolic/AS-POSS blend system ( $k = 1$ ,  $q = 25$ ) seems to have the stronger average hydrogen bonding interactions. This result may arise from two phenomena. One is that the star-shaped acetoxystyrene-POSS presents a larger fraction of hydrogen-bonded carbonyl groups than does the linear PAS, which is similar to the findings we made in a previous study of the phenolic/poly(methyl methacrylate) blend system.<sup>25</sup> The other reason is that the siloxane groups of the POSS core also take part in hydrogen bonding interactions with the hydroxyl groups of the phenolic to result in organic/inorganic polymer nanocomposites.<sup>26</sup>

## CONCLUSIONS

We have synthesized a new nanomaterial based on AS-POSS and investigated its hydrogen bonding with phenolic by using 1D and 2D FTIR spectroscopic analyses. Hydrogen bonds exist between the phenolic hydroxyl groups and both the carbonyl and siloxane groups of AS-POSS. We determined the interassociation equilibrium constant between the hydroxyl groups of the phenolic and the siloxane groups of the POSS indirectly from a least-squares fitting procedure based on the experimental fraction of hydrogen-bonded carbonyl groups in this blend system. The value of  $K_A$  (38.6) we obtained for the hydroxyl-siloxane interactions is equal to the value determined using the classical Coggeshall and Saier (C and S) methodology.

We thank the National Science Council, Taiwan, Republic of China, for supporting this research financially under Contract No. NSC-93-2216-E-009-021.

## REFERENCES AND NOTES

- Schwab, J. J.; Lichtenhan, J. D. *Appl Organomet Chem* 1998, 12, 707.

2. Lichtenhan, J. D.; Otonari, Y.; Carri, M. G. *Macromolecules* 1995, 28, 8435.
3. Shochey, E. G.; Bolf, A. G.; Jones, P. F.; Schwab, J. J.; Chaffee, K. P.; Haddad, T. S.; Lichtenhan, J. D. *Appl Organomet Chem* 1999, 13, 311.
4. Haddad, T. S.; Lichtenhan, J. D. *Macromolecules* 1996, 29, 7302.
5. Abad, M. J.; Barral, L.; Fasce, D. P.; Williams, R. J. *Macromolecules* 2003, 36, 3128.
6. Fu, B. X.; Zhang, W.; Hsiao, B. S.; Johansson, G.; Sauer, B. B.; Phillips, S.; Balnski, R.; Rafailovich, M.; Sokolov, J. *Polym Prepr* 2000, 41, 587.
7. Leu, C. M.; Chang, Y. T.; Wei, K. H. *Macromolecules* 2003, 36, 9122.
8. Mather, P. T.; Jeon, H. G.; Romo-Urbe, A.; Haddad, T. S.; Lichtenhan, J. D. *Macromolecules* 1999, 32, 1194.
9. Xu, H.; Kuo, S. W.; Lee, J. S.; Chang, F. C. *Polymer* 2002, 43, 5117.
10. Coleman, M. M.; Graf, J. F.; Painter, P. C. *Specific Interactions and the Miscibility of Polymer Blends*; Technomic: Lancaster, PA, 1991.
11. Lee, Y. J.; Kuo, S. W.; Huang, W. J.; Lee, H. Y.; Chang, F. C. *J Polym Sci Part B: Polym Phys* 2004, 42, 1127.
12. Kuo, S. W.; Chang, F. C. *Macromol Chem Phys* 2002, 203, 868.
13. Kuo, S. W.; Chang, F. C. *Macromolecules* 2001, 34, 4089.
14. Noda, I. *J Am Chem Soc* 1989, 111, 8116.
15. Ren, Y.; Murakami, T.; Nishioka, T.; Nakashima, K.; Noda, I.; Ozaki, Y. *Macromolecules* 1999, 32, 6307.
16. Makashima, K.; Ren, Y.; Nishioka, T.; Tsubahara, N.; Noda, I.; Ozaki, Y. *J Phys Chem B* 1999, 103, 6704.
17. Haung, H.; Malkov, S.; Coleman, M.; Painter, P. *Macromolecules* 2003, 36, 8148.
18. Haung, H.; Malkov, S.; Coleman, M.; Painter, P. *Macromolecules* 2003, 36, 8156.
19. Shen, Y.; Wu, P. *J Phys Chem B* 2003, 107, 4224.
20. Coggesthall, N. D.; Saier, E. L. *J Am Chem Soc* 1951, 71, 5414.
21. Coleman, M. M.; Painter, P. C. *Prog Polym Sci* 1995, 20, 1.
22. Kuo, S. W.; Huang, W. J.; Chan, S. C.; Huang, C. F.; Chang, F. C. *Macromolecules* 2004, 37, 4164.
23. Ginzburg, V. V. *Macromolecules* 2005, 38, 2362.
24. Kwei, T. K. *J Polym Sci Polym Lett Ed* 1984, 22, 307.
25. Haung, C. F.; Kuo, S. W.; Lin, H. C.; Chen, J. K.; Chen, Y. K.; Xu, H.; Chang, F. C. *Polymer* 2004, 45, 5913.
26. Xu, H.; Kuo, S. W.; Lee, J. S.; Chang, F. C. *Macromolecules* 2002, 35, 8788.